npj | clean water

www.nature.com/npjcleanwater

REVIEW ARTICLE OPEN

A review of advances in freeze desalination and future prospects

Abdul Najim[1] ✉

Freeze desalination (FD) has several benefits compared to vaporization-based and membrane-based desalination methods. The FD process needs approximately 1/7th of the latent heat required by the vaporization-based desalination processes. The involvement of sub-zero temperature in FD reduces the risk of corrosion and scaling. This paper reviews the advances in FD methods involving stand-alone and hybrid methods that operate with and without utilizing the energy released during the re-gasification of liquefied natural gas. Moreover, the paper discusses the future focus areas for research and development to make FD a commercially feasible technology. Potable water was produced from brackish water and seawater by FD wherein the nucleation was achieved by ice seeding, the mixing of rejected salt from ice into the liquid phase was controlled appropriately, growth of ice crystals was slow, and liquid subcooling was maintained at approximately 4 K. The post-treatment of obtained ice is needed to produce potable water if the process is instigated without ice seeding. The plant capacity of stand-alone progressive FD was higher than the stand-alone suspension FD of seawater. The integration of the falling-film, fractional thawing, and block FD method showed significantly improved plant capacity than the stand-alone suspension FD method. The energy consumption of stand-alone PFC and SFC-based desalination with latent heat recovery was reported close to the reverse osmosis (RO) method. The hybrid (integration of the suspension FD method with membrane distillation) FD method utilizing LNG cold energy consumed less energy than the conventional RO method.

npj Clean Water (2022)5:15 ; https://doi.org/10.1038/s41545-022-00158-1

INTRODUCTION

Water is categorized into five principal classes—(a) freshwater (0.05 wt% and less salinity); (b) brackish water (0.05–3 wt% salinity); (c) saline water (3–5 wt% salinity); (d) seawater (3.5 wt% salinity), (e) brine water (5 wt% and more salinity). Freshwater paucity is on the rise in many countries of the world because of the rapid depletion of ground and surface water[1]. The apparent answer to the worldwide water shortfall is the desalination since 97.5% of water available on Earth's surface is salty. Desalination is a promising option that addresses the water shortage by processing the salty water to drinkable water. The gross world-wide operating capacity of desalination plants is 95.37million m^3/day of fresh water[2]. Seawater desalination contributes 59%, followed by brackish water 23%, river water 7%, waste water 5%, and other sources 6%[3]

Desalination methods can be classified into two categories—(1) includes phase-change of saline water (vaporization and freezing), (2) excludes phase-change of saline water. The first category of desalination methods incorporates multieffect distillation (MED), adsorption desalination (AD), multistage flash distillation (MSF), mechanical vapor compression (MVC), humidification-dehumidification (HDH), membrane distillation (MD), and freeze desalination (FD). The second category of desalination methods concerns reverse osmosis (RO), forward osmosis (FO), capacitive deionization (CDI), ultrafiltration (UF), nanofiltration (NF), and electrodialysis (ED). Table 1 summarizes the experimental data on plant capacity, energy consumption, cost, operating temperature, environmental impact, and CO_2 emission linked with different desalination methods[3–14]. The energy consumption and cost of potable water production is less for second category desalination methods due to the absence of the phase change process. Similar trends can be observed for potable water production capacity and CO_2 emission. It is important to note that the conventional desalination methods (MED, MSF, MVC, HDH, MD, and RO) have a severe environmental impact in terms of seawater temperature, and salinity. The brine discharge increases seawater temperature and salinity significantly[3].

Freeze-concentration (FC) based desalination of saltwater is also referred to as freeze desalination (FD). The process produces ice crystal/crystals and concentrated saltwater. Freshwater is obtained by the separation of ice crystal/crystals from the concentrated saltwater and afterwards melting it. The by-product of FD is concentrated saltwater (for freeze concentration-based desalination) or salt crystals (for eutectic freezing-based desalination). Thermodynamically, the latent heat of freezing and vaporization of water is 330 kJ/kg and 2256 kJ/kg, respectively. The FD process needs approximately 1/7th of the energy required by the vaporization-based desalination processes. The insensitiveness to the fouling is another important benefit of FD compared to the membrane-based desalination processes, which typically are prone to fouling and require frequent maintenance[15]. In the case of excessive fouling, the cleaning of membranes is very difficult. There is no need for intensive pretreatment of the saltwater for FD[15]. The involvement of sub-zero temperature in FD reduces the risk of corrosion and scaling[16]. Furthermore, both vaporization and membrane-based desalination methods produce concentrated brine, which causes environmental damage. FD can treat concentrated brine close to zero liquid discharge either stand-alone[17] or integrating with membrane distillation and crystallization[18].

The FC process increases the concentration of an aqueous solution by separating the dissolved solute from ice into the liquid, undergoing crystallization. The solute separation is because the

[1]Department of Mechanical Engineering, Indian Institute of Technology Bombay, 400076 Mumbai, India. ✉email: abdulnazim219@gmail.com

Table 1. Experimental data on potable water production capacity, energy consumption, cost, operating temperature, environmental impact, and CO_2 emission linked with different desalination methods[3–14].

Desalination method	Type of saltwater	Plant capacity (m^3/h)	Electrical energy consumption (kWh_{ele}/m^3)	Thermal energy consumption (kWh_{th}/m^3)	Cost (US $/$m^3$)	Operating temperature (°C)	Environmental impact	CO_2 emission (kg/m^3)
RO	Seawater ($C_{l,0} = 3.5wt\%$)	40–13,000	5.1–7.5	Not applicable	0.5–1.7	Ambient	Brine discharges at ambient temperature, and TDS increases by 50–80%.	1.7–2.8
RO	Brackish water ($C_{l,0}$<$3wt\%$)	0.5–1600	2–5	Not applicable	0.3–0.5	Ambient	Concentrated saltwater discharges at ambient temperature, and TDS increases by 50–80%.	1.7–2.8
FO	Brackish water ($C_{l,0}$<$3wt\%$)	0.5–1000	3–8	Not applicable	0.2–0.6	Ambient	Concentrated saltwater discharges at ambient temperature.	N. A.
ED	Brackish water ($C_{l,0}$<$0.5wt\%$)	4–850	2.6–23	Not applicable	0.6–1.05	Ambient	Concentrated saltwater and brine discharges at ambient temperature.	N. A.
MVC	Seawater ($C_{l,0} = 3.5wt\%$)	250–1250	7–12	Not applicable	0.7–1.1	65–70	Brine discharge is 10–15 °C hotter than ambient, and TDS increases by 15–20%.	7.0–17.6
MED	Seawater ($C_{l,0} = 3.5wt\%$)	5–13,000	12–19	40–65	1.1-2.0	65–70	Brine discharge is 10–15 °C hotter than ambient, and TDS increases by 15–20%.	7.0–17.6
MSF	Seawater ($C_{l,0} = 3.5wt\%$)	950–22,000	20–27	53–70	1.9–2.5	90–110	Brine discharge is 10-15 °C hotter than ambient, and TDS increases by 15–20%.	15.6–25.0
MD	Brackish water ($C_{l,0}$<$3wt\%$) and Seawater ($C_{l,0} = 3.5wt\%$)	0.1–17	35–40	80–100	3.2–3.7	60–90	Concentrated saltwater and brine discharge is 10–15 °C hotter than ambient, and TDS increases by 15–20%.	7.0–17.6
HDH	Seawater ($C_{l,0} = 3.5wt\%$)	0.4–1.1	40–60	100–200	3.7–5.6	65–70	Brine discharge is 10–15 °C hotter than ambient, and TDS increases by 15–20%.	7.0–17.6

Note: N. A. Not available.

ice crystal lattice has small dimension that rejects solute ions[19]. Additionally, the solute separation mechanism from the ice phase could be due to the insignificant solubility of solute ions in the ice phase compared to water[20]. If the separated solute is not mixed into the liquid, then a high solute concentration layer builds up adjacent to the moving ice-liquid interface. As the layer grows, the solute gets trapped into the ice by the ice-liquid interface[21]. This increases the concentration of the solute into the ice and severely affects its purity. Figure 1(a) and (b) show the schematic of the concentration profile with diffusional and convective mixing of the rejected solute in the liquid, respectively. In Fig. 1(a) and (b), C_s is the salinity of the ice (wt%), C_l is the salinity of the concentrated liquid (wt%), $C_{l,0}$ is the initial salinity of the liquid (wt%), and δ is the thickness of the concentration boundary layer (mm). Mixing of the rejected solute into the liquid is obligatory to reduce its trapping into the ice. It shrinks the concentration layer adjacent to the moving ice-liquid interface. Mixing can be achieved by creating liquid movement near the ice-liquid interface. In practice, continuous rejection of the solute at the ice-liquid interface results in a formation of a static boundary layer[19]. Hence, a complete shrinking of the boundary layer is unlikely. The growth rate of an ice crystal affects its purity[22]. An ice crystal grows in columns at a lower growth rate, resulting in a flat ice-liquid interface, and the salt separates easily. At a higher growth rate, an ice crystal grows in the form of dendrite. The salt gets trapped easily in the dendrite arm and severely affects the ice purity. The ice seeding decreases the supercooling of the liquid and promotes the formation of an ice crystal in columns[19,23]. This increases the purity of ice. A higher degree of supercooling promotes the formation of dendritic ice structure, decreasing its purity.

FC is classified into direct contact and indirect contact methods. Figure 2 depicts the schematic of the direct contact FC process. The process uses a volatile secondary refrigerant of a refrigeration cycle[24]. The cold liquid refrigerant is mixed directly with the saltwater in a crystallizer where refrigerant evaporation occurs due to heat transfer from saltwater. The saltwater gets frozen in the form of ice crystals suspended in the concentrated saltwater. The ice crystals are separated from the concentrated saltwater and sent for post-treatment (for example, washing). Freshwater is obtained by melting post-treated ice crystals. The refrigerant is recycled into the crystallizer. The post-treatment of ice crystals is necessary because the salt present in the concentrated liquid can contaminate the ice crystals[25]. In the indirect FC process, a wall separates the saltwater and refrigerant (coolant). The indirect contact FC process is classified into suspension freeze-concentration (SFC) and layer freeze-concentration. These methods are investigated by researchers for application in fruit juices[26,27], glucose solution[28], dairy products[29,30], pharmaceutical[31,32], and wastewater treatment[33]. During the SFC process (Fig. 3), the steps involved are nucleation, crystal growth, separation of ice crystals from the concentrated liquid, and post-treatment of ice crystals for its purity improvement. This method produces many small ice crystals suspended in a concentrated liquid. The ice crystals grow large by the Ostwald ripening mechanism[21]. A separate heat exchanger is required to produce

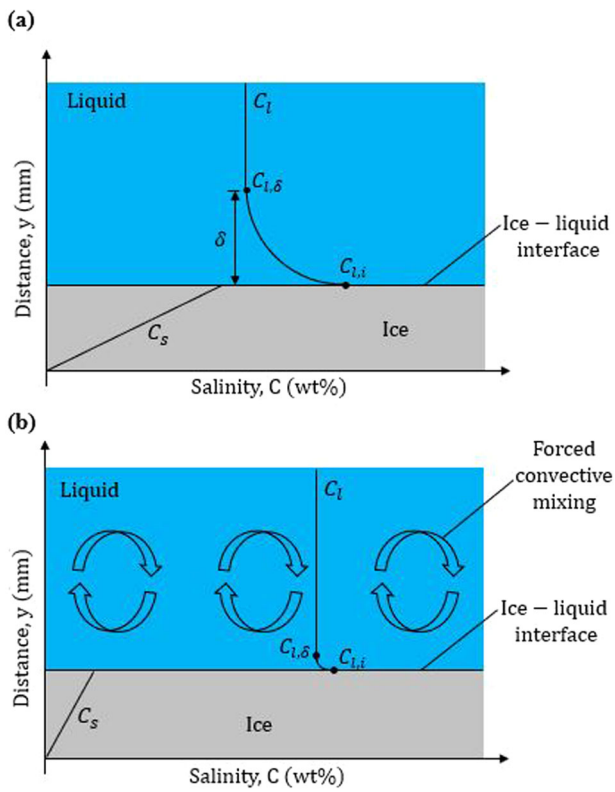

Fig. 1 Schematic of the concentration profiles during solidification of an aqueous mixture. a with diffusional mixing of the rejected solute, **b** with convective mixing of the rejected solute.

ice seeds for nucleation. Hence, SFC needs a complex system with dedicated control, making it most expensive amid other liquid concentration methods[34]. The layer-by-layer freeze-concentration process leads to forming a single and large ice crystal over the cooling surface. This process is classified into progressive freeze-concentration (PFC), falling-film freeze-concentration (FFFC) and block freeze-concentration (BFC). During the PFC process (Fig. 4), a single ice crystal is grown unidirectionally on a cooling surface with liquid movement adjacent to the ice-liquid interface. The purity of ice crystal is higher in cases of PFC compared to SFC[21,34]. Furthermore, the separation of ice crystal from the liquid is easy compared to SFC. The concentrated liquid is removed after the process. This leaves only ice crystal inside the crystallizer. The ice crystal is removed from the crystallizer after melting. The elimination of a heat exchanger (for the production of ice seeds) and ice crystal separation equipment reduces the system's complexity. Moreover, it also reduces operation and maintenance costs[35]. Fig. 5 shows the schematic of the FFFC process. The aqueous liquid to be concentrated flows down over the cooling surface. The crystallization of the aqueous mixture occurs over the cooling surface as the cooling surface temperature is maintained sufficiently below the liquidus temperature of the aqueous mixture[36]. The ice sticks to the cooling surface while the concentrated liquid flows down the cooling surface. A single layer of ice forms on the cooling plate, and the concentrated liquid is re-circulated continuously. The process with multiple plates increases the product yield drastically[37]. The process can handle the aqueous liquid with a high solute concentration[38]. Fig. 6 depicts the schematic of the BFC process. The stagnant aqueous solution is completely frozen in the BFC method and then partially thawed. The heating bath facilitates the partial thawing of the ice block. BFC process can handle the aqueous liquid with a low solute concentration[38]. The FFFC and BFC

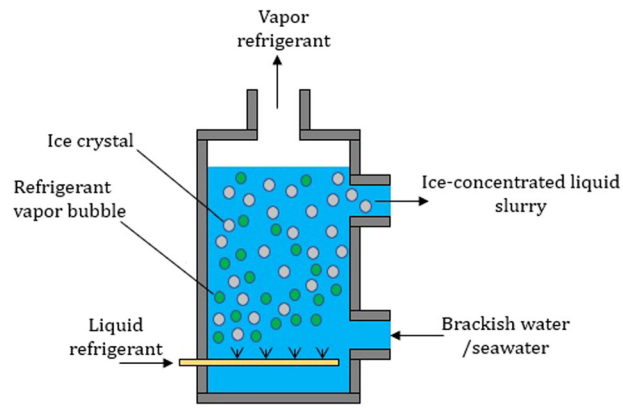

Fig. 2 Schematic of the direct contact freeze-concentration process. The cold liquid refrigerant is mixed directly with the saltwater in a crystallizer where refrigerant evaporation occurs due to heat transfer from saltwater.

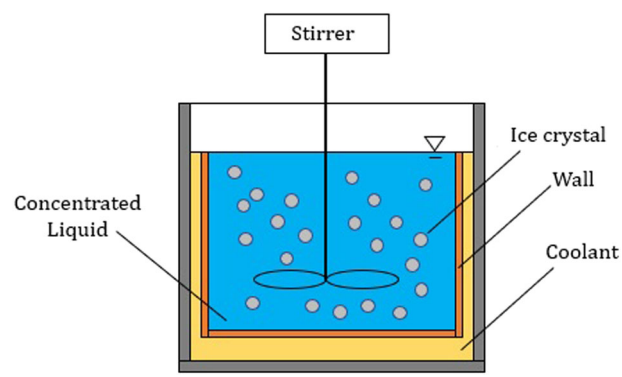

Fig. 3 Schematic of the suspension freeze-concentration process. The method produces many small ice crystals suspended in a concentrated liquid.

method is also known as dynamic layer freeze-concentration and static layer freeze-concentration, respectively.

The efficiency of a FC system is evaluated based on the effective partition constant (K_{eff})[21,34]. K_{eff} is defined as the ratio of the concentration of the solute in the ice phase (C_s) to the concentration of solute in the liquid phase (C_l). Mathematically, K_{eff} is expressed as:

$$K_{eff} = \frac{C_s}{C_l} \tag{1}$$

The value of K_{eff} varies between 0 and 1. A lower value (close to 0) indicates ice crystals with high purity, and a higher value (close to 1) indicates low purity. The separation of solute from the aqueous solution increases with decreasing K_{eff}. Thus, the purity of the ice and efficiency of the process increases with decreasing K_{eff}. The value of K_{eff} can be obtained from the mass balance of the solute[21,34] as:

$$K_{eff} = 1 - \frac{\ln\left(C_{l,0}/C_l\right)}{\ln\left(V_l/V_{l,0}\right)} \tag{2}$$

where, V_l is the volume of the concentrated liquid (m^3) and $V_{l,0}$ is the initial volume of the liquid (m^3).

For aqueous solutions like saltwater, phase change takes place between the liquidus and solidus temperatures. The presence of salt reduces the liquidus temperature of the mixture. The phenomenon is known as freezing point depression[39], which is

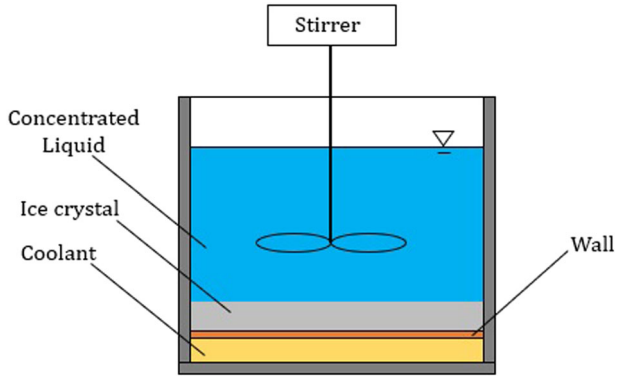

Fig. 4 Schematic of the progressive freeze-concentration process. A single ice crystal is grown unidirectionally on a cooling surface with liquid movement adjacent to the ice-liquid interface.

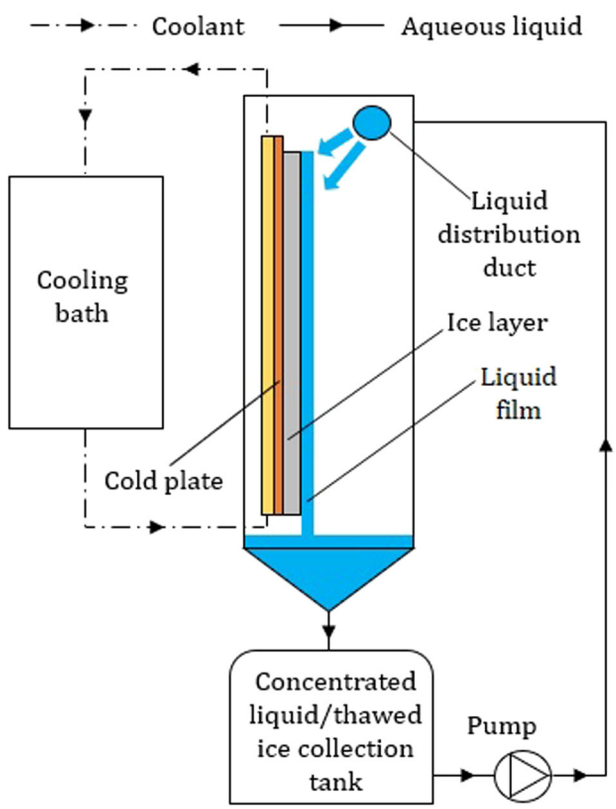

Fig. 5 Schematic of the falling-film freeze-concentration process. The aqueous liquid to be concentrated flows down over the cooling surface where the crystallization occurs.

expressed as:

$$\Delta T_{fpd} = -ab\phi \quad (3)$$

where, a is the van't Hoff factor linked to the number of ion particles (for NaCl, a=2), b is the cryoscopic or molal depression constant (for water, b=1.853K·kg/mol), and ϕ is the molality of the saltwater (mole of NaCl/kg of water). It is important to note that the liquidus temperature of saltwater is dependent on the salt concentration in the mixture[40]. As the freeze-concentration of NaCl-H_2O mixture proceeds, the salt concentration in the liquid phase increases. This leads to a further reduction in the liquidus temperature. Figure 7 shows the schematic of the NaCl-H_2O mixture equilibrium phase diagram[41]. Consider the saltwater 'A' having sub-eutectic concentration and maintained at a

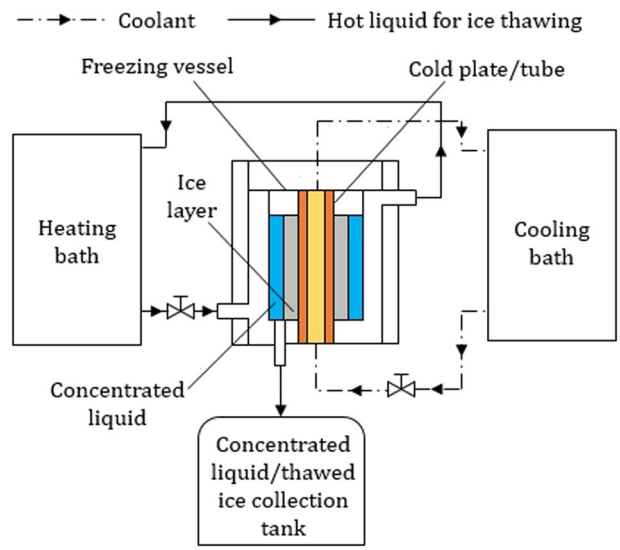

Fig. 6 Schematic of the block freeze-concentration process. The stagnant aqueous solution is completely frozen and then partially thawed.

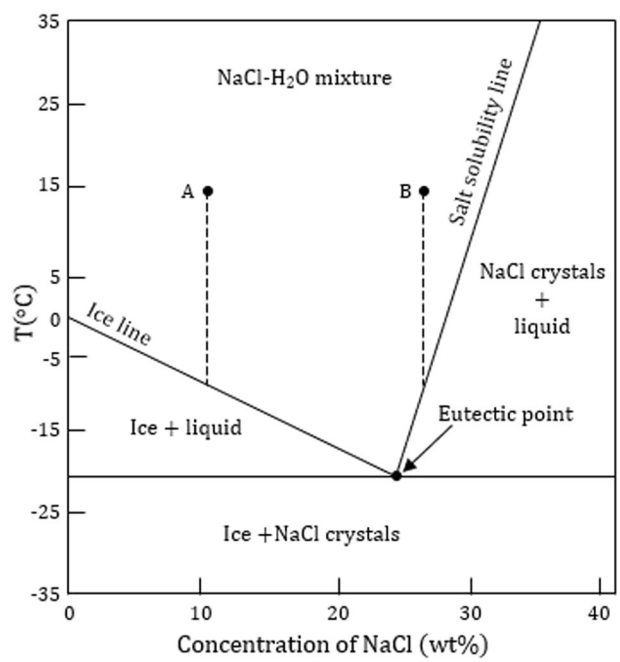

Fig. 7 NaCl-H_2O mixture equilibrium phase diagram[41]. The solidification of the NaCl-H_2O mixture follows the ice line or salt solubility line depending on the initial salinity.

sub-eutectic temperature. As the freeze desalination process progresses, the mixture reaches the liquidus line (also known as the ice line), and ice formation begins. If the saltwater 'B' having hypereutectic concentration and maintained a sub-eutectic temperature is cooled down, it reaches the solubility line, and salt crystal formation begin. It necessary to emphasize that if salt crystal forms first, the process is called as cooling crystallization and not freeze-concentration due to the absence of ice formation[42]. The eutectic point reaches upon further cooling of both 'A' and 'B'. The eutectic point represents the lowest freezing point of the mixture (-21.1°C) and the largest amount of salt (23.3 wt%) dissolved in the liquid phase[43]. The process of simultaneous ice and salt formation is referred to as Eutectic

Freeze Crystallization. During the process, ice floats in the mixture and salt crystals settle at the bottom of the crystallizer. This makes easy separation of both solid phases.

The most widely used practice to transport natural gas is to convert it into liquid. The natural gas (NG) liquefies by reducing its temperature to -162°C[44]. The liquefaction process involves a large amount of energy. The liquefied natural gas (LNG) can be easily stored and less inflammable than natural gas[45]. LNG requires to be re-gasified at the receiving station before being sent to consumers. The heat required to re-gasify the LNG is usually supplied by seawater maintained at ambient temperature[46]. As a result, a huge amount (~830 kJ/kg) of cold energy is wasted during the re-gasification process[47]. LNG cold energy is utilized for cryogenic power generation, gas (oxygen, nitrogen, helium, etc.) production from air separation, cryogenic CO_2 capture, data center cooling, cold energy storage, seawater desalination, and many more applications[48].

This paper reviews the advances in stand-alone and hybrid FD methods operating with and without utilizing LNG cold energy. The performance of a FD method is evaluated based on salinity of the product ice, salinity of the concentrated liquid, salt removal efficiency, water recovery efficiency, potable water production capacity, energy consumption, and cost. The objective of the paper is to review the scientific articles on freeze desalination published from 2011 to 2021 and propose the future focus areas for research and development to make freeze desalination a commercially feasible technology. The history and state-of-the-art concerning freeze desalination have been covered extensively elsewhere[42,43].

STAND-ALONE AND HYBRID METHODS THAT OPERATE WITHOUT UTILIZING LNG COLD ENERGY

This section provides the performance of stand-alone and hybrid FD methods operating without utilizing LNG cold energy. Here, the hybrid FD method refers to the integration of FD with other desalination methods such as MD and RO. The performance is assessed on the basis of salinity of the product ice (C_s), the salinity of the concentrated saltwater (C_l), salt removal efficiency (S), and water recovery efficiency (W). A separate section (5) is added to discuss the performance of FD methods on the basis of potable water production capacity, energy consumption, and cost. The values of S and W were determined by using the following equations:

$$S = \frac{C_{l,0} - C_s}{C_{l,0}} \times 100 \quad (4)$$

$$W = \frac{V_s - V_{seed}}{V_{l,0}} \times 100 \quad (5)$$

where, V_s is the volume of thawed ice (m^3), V_{seed} is the volume of seed ice (m^3), $V_{l,0}$ is the initial volume of the saltwater (m^3), $C_{l,0}$ is the initial salinity of the saltwater (wt%), and C_s is the salinity of thawed ice (wt%).

Direct contact FD

The volatile refrigerant such as butane creates a severe safety issue during the direct contact FD process because of their explosive nature[24]. Erlbeck et al.[49] carried out an experimental investigation of direct contact FD of seawater using non-volatile refrigerants (Cassida Fluid DC20 and Solkatherm® SES36). They addressed the safety issue successfully. However, the ice gets contaminated heavily compared to the volatile refrigerant. The ice salinity (C_s) was found to be 2.64 wt% and 2.56 wt% for experiments with Cassida Fluid DC20 and Solkatherm® SES36, respectively. Liu et al.[50] studied spray freezing for seawater desalination ulitlizing free cold energy from the cold atmosphere mathematically. A 200 m high desalination tower was proposed to generate 27.7 kg/s potable water from seawater at an atmospheric temperature of −26°C. Furthermore, the method can produce potable water and generate green power simultaneously.

FD based on suspension freeze-concentration

Table 2 summarizes the performance of different experimental studies involving SFC-based desalination method operates without utilizing LNG cold energy.

FD based on progressive freeze-concentration

Table 3 summerizes the performance of various experimental studies linked to PFC based desalination method operates without utilizing LNG cold energy.

FD based on falling-film and block freeze-concentration methods

Williams et al.[61] studied FD of Arabian Gulf seawater and RO brine based on the FFFC process using the modified ice maker machine. The crystallization time, initial salinity of the saltwater, and the saltwater flow rate were the parameters that affect the process. The salinity reduction for RO brine using multistage processing was achieved as 39.3%. Zambrano et al.[62] presented an innovative combination of falling-film freeze-concentration, fractional thawing (FT), and block freeze-concentration to produce potable water from seawater. Ice crystals obtained from the falling-film freeze-concentration unit was supplied to the fractional thawing unit, while the brine was dispensed to another falling-film freeze-concentration unit. The fractional thawing unit produced thawed ice. The brine was supplied back to the falling-film freeze-concentration unit, and thawed ice was supplied to a block freeze-concentration unit. The concentrated brine obtained from the block freeze-concentration unit was supplied back to the initial falling-film freeze-concentration unit. The third stage of the block freeze-concentration unit produced potable water. The combination of falling-film freeze-concentration and fractional thawing with five steps and block freeze-concentration with three steps were reported to get a salinity reduction of 98.5%.

Hybrid systems

No experimental study on hybrid systems involving the integration of FD with other desalination methods was found in the literature. However, few studies[63,64] explored the integration of FD with other desalination methods (RO and humidification) mathematically. Baayyad et al.[63] proposed a combination of FD with RO to reduce the energy consumption for seawater desalination. The SFC-based FD successfully pretreated seawater for the RO modules. As a result, the energy consumption and quality of freshwater were improved by approximately 25% and 71%, respectively, compared to the conventional RO desalination process. Han et al.[64] proposed a mathematical model for the humidification-FD hybrid system based on the mass and energy equilibrium for seawater desalination. Here, the SFC-based FD was selected for the study. The authors concluded that the humidification-FD hybrid system can only operate at the air mass flow rate in the range of 24.41-25.47 kg/s because of the constraint from the wet-bulb temperature of air and the fixed arrangement.

STAND-ALONE AND HYBRID FD METHODS UTILIZING LNG COLD ENERGY

Direct contact FD

Xie et al.[65] developed an ice generator based on the direct contact FD process using the cold energy from re-gasification of LNG. Here, the recirculating refrigerant was non-volatile and immiscible.

Table 2. Experimental studies concerning stand-alone SFC-based desalination method that operates without utilizing LNG cold energy.

Reference	Equipment	Mode of operation	Type of Saltwater	Salinity of ice, C_s (wt %)	Salinity of concentrated liquid, C_l (wt%)	Salt removal efficiency, S (%)	Water recovery efficiency, W (%)	Technique to enhance the ice purity	Other findings
Erlbeck et al.[49]	Stirred cylindrical crystallizer cooled laterally	Batch	Brackish water ($C_{l,0} = 1wt\%$)	0.01	N. A.	99	22	Ice pressing	• Intense stirring decreased the rate of ice formation.
Zvinowanda et al.[51]	HybridICE™ unit including a refrigeration unit and scraped surface heat exchangers	Batch	Brackish water ($C_{l,0} = 1.47wt\%$)	0.04	2.24	97.5	50	N. A.	• The ice yield was inversely proportional to the liquid circulation flow rate and scrapper motor speed.
		Continuous	Brine ($C_{l,0} = 4.92wt\%$)	1.7	7.08	82.8	34		
Erlbeck et al.[52,53]	Screw based scraped surface heat exchanger with ice pressing unit	Batch	Seawater ($C_{l,0} = 3.5wt\%$)	0.01	N. A.	99.7	N. A.	Ice pressing	• Salinity reduction for seawater reached above 99% at the subcooling of approximately 4 K. • The optimum force to press ice and holding time was found to be 37.4kN and 180 s, respectively.
Shin et al.[54]	Scraped surface heat exchanger	Batch	Seawater ($C_{l,0} = 3.5wt\%$)	0.18	5	94.9	40	Washing	• Ice seeding was not required for producing irrigation water.
Sahu et al.[55]	U-shaped scraped surface crystallizer which integrates pre-cooling, freezing and ice removal	Continuous	Seawater ($C_{l,0} = 3.5wt\%$)	0.80	N. A.	77.1	15	Washing	• The two-step washing of ice was observed to be effectual in decreasing salinity compared to single-step washing.
Abdelmoaty et al.[56]	A cylindrical tank cooled peripherally	Batch	Brackish water ($C_{l,0} = 3wt\%$)	1.67	N. A.	44.3	15.6	N. A.	• Increase in the intensity of the magnetic field increased the ice purity by decreasing the concentration gradient near the ice-liquid interface.

Note: N. A. Not available.

Table 3. Experimental studies concerning stand-alone PFC-based desalination method that operates without utilizing LNG cold energy.

Reference	Equipment	Mode of operation	Type of Saltwater	Salinity of ice, C_s (wt %)	Salinity of concentrated liquid, C_l (wt%)	Salt removal efficiency, S (%)	Water recovery efficiency, W (%)	Technique to enhance the ice purity	Other findings
Rane and Padiya[15]	Heat pump driven tube-tube heat exchanger with the cold energy recovery	Batch	Seawater ($C_{l,0} = 3.5wt\%$)	0.05	7.0	98.6	50	N. A.	• Mass flow rate of seawater equal to 2000kg/h, operating temperature of the refrigerant in the evaporator equal to -7°C and condensing temperature equal to 3°C were determined as optimum.
Rich et al. [57]	Stainless-steel tube submerged in a glass tank with air bubbling	Batch	Seawater of Rabat, Morocco ($C_{l,0} = 3.8wt\%$)	0.03	6.2	99	18.9	Sweating	• Sweating increased the ice purity by drawing off the trapped concentrated solution pockets.
Hamid et al.[58]	Coil crystallizer	Batch	Seawater ($C_{l,0} = 3.5wt\%$)	1.3	N. A.	38	N. A.	N. A.	• Salt removal increased with saltwater circulation rate. • Optimum operating conditions are the coolant temperature equal to -10°C and saltwater circulation rate equal to 3000 ml/min.
Fujioka et al.[59]	Vertical freezing apparatus	Batch	Seawater ($C_{l,0} = 3.5wt\%$)	0.03	4.7	99	25	N. A.	• Purity of ice was decreased with increasing ice-liquid interface speed due to inadequate time for salt to mix into the liquid. • Optimum operating conditions to get potable water from seawater and brackish water are the ice-liquid interface speed equal to 0.5 cm/h and stirring speed equal to 0.96 m/s.
Moharramzadeh et al.[60]	Vertical freezing apparatus	Batch	Seawater ($C_{l,0} = 3.5wt\%$)	1.51	4.56	57	40.5	N. A.	• Salt removal efficiency was higher for the up-pumping of the liquid than the down-pumping.

Note: N. A.: Not available.

Table 4. Experimental studies concerning stand-alone SFC-based desalination method utilizing LNG cold energy.

Reference	Equipment	Mode of operation	Type of Saltwater	Salinity of ice, C_s (wt%)	Salinity of concentrated liquid, C_l (wt%)	Salt removal efficiency, S (%)	Water recovery efficiency, W (%)	Technique to enhance the ice purity	Other findings
Chang et al.[68]	A cylindrical tank cooled peripherally	Batch	Seawater ($C_{l,0} = 3.5wt\%$)	0.03	N. A.	99	26	Washing	• The coolant temperature and stirring rate to get potable water were -8°C and 200 rpm, respectively.
Lin et al.[69]	Flake ice maker	Batch	Brackish water ($C_{l,0} = 2.4wt\%$)	1.06	N. A.	55.8	N. A.	Washing	• Liquid nitrogen was selected to substitute LNG.

Note: N. A. Not available.

The refrigerant featured by a low freezing point, a high boiling point, and low toxicity. The refrigerant was injected into seawater. Ice crystals were formed on the surface of refrigerant bubbles. The refrigerant was retrieved at the base of the ice generator by means of gravity-assisted separation. The ice slurry was collected at the top of the ice generator. The apparatus effectively illustrated the separation of ice crystals and retrieval of the refrigerant. The ranges of C_s, S and W are 0.92–1.15 wt%, 83.5–80.1%, and 23–34%, respectively. Ong and Chen[66] estimated that 1 kg of LNG regasification consumes 7.83 kg of seawater and 1.66 kWh of electric energy, and produce 1.64 kg of potable water. The system is suitable for nations with low electric power rates but high potable water prices[66].

FD based on suspension freeze-concentration

Cao et al.[67] investigated SFC-based FD using an intermediate secondary refrigerant to transport the cold energy from LNG to seawater theoretically. The authors used HYSYS and gPROMS software to model the transport process and simulation. The authors evaluated that 1 kg of potable water can be obtained from seawater at the cost of 0.5 kg equivalent of LNG cold energy. Chang et al.[68] explored the previous work by carrying out experiments at the laboratory level. A cylindrical freezing unit made of stainless steel containing a stirrer was used as crystallizer. A parametric study was carried out to study the effect of intermediate refrigerant temperature, washing of ice crystals, the quantity of washing water, duration of the process, supercooling of seawater, and stirring speed on ice salinity. The water obtained from the study has met the World Health Organization (WHO) standard for potable water salinity (≤0.05 wt%) at optimum operating conditions. The amount of washing water required to get the potable water was 50 wt% of ice obtained. The authors did not report the amount of LNG required to produce potable water from seawater. Lin et al.[69] used R410A as an intermediate secondary refrigerant to transport cold energy from liquid nitrogen, which was used to simulate LNG. The authors conducted an experimental study by using a flake ice maker as the freezing unit. A parametric study was conducted to investigate the effect of refrigerant evaporating temperature, the quantity of spray nozzles, and the seawater flow rate on the salinity of water produced during the process. The salinity reduction of approximately 50% was obtained at the optimum working conditions. The amount of LNG required to produce potable water from seawater is consistent with the study of Cao et al.[67] Table 4 presents the performance of different experimental investigations associated with SFC based desalination utilizing LNG cold energy.

Hybrid systems

Wang and Chung[70] demonstrated the combination of SFC-based FD and membrane distillation (MD) for seawater desalination experimentally. The seawater was first treated by FD, producing potable water from the obtained thawed ice. The bi-product of the FD process was treated by direct contact MD, resulting in its further concentration. The direct contact MD process produced potable water as the main product. The authors used an heat exchanger to supply cold energy to both the FD crystallizer and the direct contact MD method. The water recovery efficiency of 71.5% was attained at optimum operating conditions. The direct contact MD process in the previous study is replaced by vacuum membrane distillation by Chang et al.[71] Furthermore, the electricity required for the operation of the hybrid system was fulfilled by harvesting solar energy. In this case, the water recovery efficiency was improved to 74%. Table 5 presents experimental investigations associated with hybrid FD methods utilizing LNG cold energy. Lu et al.[72] investigated a hybrid system comprising the integration of SFC-based FD and membrane distillation crystallization (MD-C) mathematically. MD-C combines direct

Table 5. Experimental studies concerning hybrid FD methods employing LNG cold energy.

Reference	Method	Individual unit	Type of Saltwater	Salinity of ice, C_s (wt %)	Salinity of concentrated liquid, C_l (wt%)	Salt removal efficiency, S (%)	Water recovery efficiency, W (%)	Technique to enhance the ice purity	Other findings
Wang and Chung[70]	Integration of SFC based FD and direct contact membrane distillation	SFC based FD	Seawater ($C_{l,0} = 3.5wt\%$)	0.02	4.19	99	18.25	Ice seeding	• The water recovery efficiency was much higher than the conventional seawater RO desalination method.
		Direct contact MD	Brine ($C_{l,0} = 4.19wt\%$)	0.01	N. A.	99	53.25	Not applicable	
Chang et al.[71]	Integration of SFC based FD and vacuum membrane distillation	SFC based FD	Seawater ($C_{l,0} = 3.5wt\%$)	0.02	4.6	99	74	Washing	• Photovoltaic panels fulfilled the electricity required for the operation of the hybrid system by harvesting solar energy.
		vacuum MD	Brine ($C_{l,0} = 4.6wt\%$)	0.01	N. A.	99		Not applicable	

Note: N. A.: Not available.

contact MD and salt crystallization to produce potable water and recover costly minerals in the crystallized form[73]. As explained in the previous study, seawater was first sent to FD unit, producing freshwater and brine. The brine is treated by direct contact MD, producing freshwater and concentrated brine. The concentrated brine was supplied to the cooling crystallizer, producing salt and ice crystals and achieving zero liquid discharge. The re-gasification of LNG supplied the cooling energy required for cooling crystallization. FD-MD-C system produced potable water with a high water recovery efficiency (>74%). Moreover, zero waste generation and salt recovery are noteworthy benefits of the system. It is important to note that the authors[70–73] preferred SFC-based FD to integrate with other desalination methods. No experimental or mathematical study on the integration of PFC, FFFC, and BFC-based FD with other desalination methods is reported in the literature.

Integration of FD method with electric power generation plant utilizing LNG cold energy

Stirling cycle, Kalina cycle, Rankine cycle, Brayton cycle, and absorption cycle have been used to generate electric power utilizing LNG cold energy[48]. Eghtesad et al.[74] stated that the utilization of entire LNG cold energy for power generation is not the most efficient way of harnessing it since the efficiency of a power generation cycle decreases at a higher temperature of LNG. The authors proposed a new power generation cycle integrated with a seawater FD system to utilize the LNG cold energy efficiently. A part of LNG cold energy is extracted at the exit of the power cycle to run the BFC-based seawater FD system. At optimum operating conditions, the proposed cycle improved the power generation by 5.7% with 0.53 kg of ice in the FD system. The authors did not provide data on key FD parameters like salinity of the product ice (C_s), the salinity of the concentrated saltwater (C_l), salt removal efficiency (S), water recovery efficiency (W), potable water production capacity, and energy consumption.

POST-TREATMENT OF THE ICE AND BRINE MANAGEMENT

Post-treatment of the ice

Washing[51,54,55,67–69,75,76], sweating[57,76–78] and centrifuging[49,76,79–81] methods are commonly used for post-treatment for the FD (stand-alone/hybrid) methods to enhance the water quality by separating the concentrated liquid from the ice. Han et al.[76] reported that washing, sweating, and centrifuging improved the salt removal to 93%, 95%, and 98%, respectively. The amount of freshwater required to get potable water by washing ranges from 40% to 50 wt% of the ice obtained after SFC based process[54,55,68]. It is important to note that a large amount of freshwater is required to get potable water from the ice by washing. Hence, FD plants using washing as a post-treatment process are not economically feasible, and no working plants are installed besides research plants[82]. Centrifuging performs slightly better in salinity reduction than washing and sweating methods. However, centrifuging could be too expensive for a pilot-scale plant[76]. Erlbeck et al.[52,53] demonstrated the ice pressing as a novel method for post-treatment of the ice to enhance the water quality. Ice pressing improved the salt removal to 98%, which is consistent with centrifuging. The concentrated liquid is forced to drain out while pressing the obtained ice, leaving only the ice with reduced salinity. The required pressing force was nominal enough to avert the loss through melting[52]. Tang et al.[83] showed that the microwave treatment could improve the water quality produced from seawater during the block FD process. Under microwave heating of ice, the trapped concentrated liquid rapidly warm up to melt the cell wall. This accelerates the formation of concentrated liquid channels and releases the concentrated liquid out of the ice. The salt removal was reached up to 90% using microwave heating. Water quality was observed to be enhanced further by combining microwave heating with centrifuging[84].

Brine management

Brine is the by-product of a desalination process (both distillation and membrane-based). It is an aqueous mixture having high concentration of NaCl and other chemical contaminants such as HCl, $AlCl_3$, NaOCl, $NaHSO_3$, H_2SO_4, and $FeCl_3$[85]. The density of brine is higher than brackish water and seawater. Consequently, brine disposal contaminates the marine environment. Sea disposal, land disposal, and deep well injection of brine create severe environmental concerns[86]. Many methods (the evaporation pond, membrane distillation, forward osmosis, electrodialysis, and capacitive deionization) have been developed for brine treatment[87,88]. The evaporation pond is effective only in an area with arid[43]. Membrane-based methods are always prone to fouling[90]. FD based on eutectic freezing can treat brine effectively[89,90]. The process involves the simultaneous formation of ice and salt crystals. Their separation takes place due to their density difference. FD based on eutectic freezing is a potential method of mineral (sodium, magnesium, calcium, potassium, lithium, thorium, and uranium) recovery from seawater[43,91]. This could lead to a reduction in the cost of potable water production from seawater.

POTABLE WATER PRODUCTION CAPACITY, ENERGY CONSUMPTION, AND COST

Estimation of energy consumption and cost

The thermal energy released during FD of saltwater ($e_{th,tot,m}$) is the sum of sensible heat released during cooling of saltwater from ambient temperature to its liquidus temperature ($e_{sens,1,m}$), latent heat of freezing of saltwater ($e_{lat,m}$), and sensible heat liberated to stabilize the ice structure during freezing ($e_{sens,2,m}$)[92]. The values of $e_{sens,1,m}$, $e_{lat,m}$, and $e_{sens,2,m}$ can be computed by using subsequent equations:

$$e_{sens,1,m} = \left(c_{p,l,amb}T_{l,amb} - c_{p,l,liq}T_{l,liq}\right), \mathrm{kJ/kg} \tag{6}$$

$$e_{lat,m} = H_{ls}, \mathrm{kJ/kg} \tag{7}$$

$$e_{sens,2,m} = c_{p,s}\left(T_{l,liq} - T_{cool}\right), \mathrm{kJ/kg} \tag{8}$$

where, $m_{l,0}$ is the initial mass of the saltwater (kg), $c_{p,l}$ is the specific heat of the saltwater (kJ/kg-K), T_l is the temperature of the saltwater (°C), m_s is the mass of the ice (kg), H_{ls} is the latent heat of freezing of the saltwater (kJ/kg), $c_{p,s}$ is the specific heat of the ice (kJ/kg-K), $T_{l,liq}$ is the liquidus temperature corresponding to the salinity of the liquid (°C), and T_{cool} is the coolant temperature (°C). The subscripts *th*, *sens*, *lat*, *m*, 0, *l*, *s*, *liq*, and *cool* represent thermal, sensible, latent, mass, initial, saltwater, ice, liquidus, and coolant, respectively. The equation to calculate $T_{l,liq}$[93] is expressed as:

$$T_{l,liq} = T_{pw} - ab\emptyset, {}^{\circ}\mathrm{C} \tag{9}$$

where, T_{pw} is the freezing temperature of the pure water (°C). $T_{l,liq}$ in Eqs. (6) and (8) corresponds to the initial ($C_{l,0}$) and final salinity of the saltwater (C_l), respectively. The values of $c_{p,l}$, $c_{p,s}$ and H_{ls} as a function of salinity and temperature can be calculated by using the equations proposed by Yen[94]. The electrical energy consumption ($e_{ele,1,m}$) to achieve $e_{th,tot,m}$ can be computed as:

$$COP = \frac{e_{th,tot,m}}{e_{ele,1,m}} \tag{10}$$

where, *COP* is the coefficient of performance of a refrigeration cycle. The subscripts *ele* and *tot* represent electrical and total, respectively. The electrical energy consumption per unit volume of potable water produced ($e_{ele,1,V}$) can be computed as:

$$e_{ele,1,V} = \frac{e_{ele,1,m} \times 1000}{3600}, \mathrm{kWh_{ele}/m^3} \tag{11}$$

The total electrical energy consumption per unit volume of potable water produced ($e_{ele,tot,V}$) can be calculated as:

$$e_{ele,tot,V} = e_{ele,1,V} + e_{ele,2,V}, \mathrm{kWh_{ele}/m^3} \tag{12}$$

where, $e_{ele,2,V}$ is the electrical energy consumed by different types of equipment like a pump, stirrer, electric motor, heating bath etc. The cost to produce 1m^3 of potable water (R) can be computed as:

$$R = e_{ele,tot,V} \times P, \mathrm{US\$/m^3} \tag{13}$$

where, P is the price of electricity per unit (US$/kWh).

Potable water production capacity, energy consumption and cost

The data on potable water production capacity, energy consumption, and the cost for different FD methods reported in the literature is limited. Table 6 shows the potable water production capacity, energy consumption, and cost data for the different FD methods. From Tables 1 and 6, it is clear that the potable water production capacity is low for the FD methods compared to other desalination methods (RO, FO, MD, ED, MSF, MVC, MED, and HDH). The slow growth rate of ice crystals[49,59] resulted in low plant capacity. Furthermore, most of the FD investigations are limited to laboratory-scale experiments. Most other desalination methods (RO, MSF, MVC, MED, and HDH) are well-established technologies and have been operating commercially for decades. For stand-alone SFC and PFC based FD operating without utilizing LNG cold energy, the maximum plant capacity was 0.042 m^3/h and 1 m^3/h, respectively. The high plant capacity of PFC based FD is attributed to increased heat transfer surface area. The integration of FFFC, FT, and BFC based FD system operationg without using LNG cold energy has a higher plant capacity than stand-alone SFC based FD systems. The electrical energy consumption and cost of potable water production for SFC based FD method without latent heat recovery was less than MD and HDH methods, similar to the MED and MSF methods, and higher than the membrane-based desalination method without phase change. In several studies, the latent heat of freezing is recovered by integrating hot and cold process streams[15,96] and reducing the operating temperature of the condenser of a refrigeration cycle[62]. Many studies[65,68–71] utilized LNG cold energy to extract latent heat of freezing and sensible heat energy from seawater. The electrical energy consumption and cost for a stand-alone SFC and PFC based FD method with latent heat recovery[15,62,96] and a hybrid (integrating MD and SFC based FD) method utilizing LNG cold energy[70] improved drastically. The energy consumption and cost are close to the conventional RO method in several studies[15,62,96]. Moreover, one study[70] reported that the energy consumption and cost are less than the conventional RO method. It is important to mention that the common practice of reporting energy consumption in FD methods utilizing LNG cold energy may be erroneous. An accurate approach would be to report the total energy consumption of the FD process and report the portion of that energy supplied by LNG re-gasification.

Estimation of energy consumption based on the standard primary energy approach

The method of energy consumption estimation and concerning data reported in sections 5.1 and 5.2 is based on derived energy, such as electricity which is susceptible to the conversion losses of power plants. As derived energies (electrical, thermal, and renewable) are usually expressed by the units, either kWh or Joule, these units cannot accurately differentiate the grade of energy supplied to the processes[98]. This causes a misconception in the evaluation of energy efficiency[98–102]. The standard primary energy approach[98–102] accurately estimates the energy efficiency of a desalination system. The approach is simple, practical and

Table 6. Experimental data on potable water production capacity, electrical energy consumption and operating cost for different FD methods.

Reference	FD method	Type of saltwater	Use of LNG cold energy	Plant capacity (m^3/h)	Energy consumption (kWh_{ele}/m^3)	Cost (US$/$m^3$)
Erlbeck et al.[53]	Stand-alone SFC based FD	Seawater ($C_{i,0} = 3.5wt\%$)	No	N. A.	30.7	2.9
Mtombeni et al.[95]	Stand-alone SFC based FD	Brackish water ($C_{i,0} = 1.47wt\%$)	No	0.042	21–26	2–2.4
Chen et al.[96]	Stand-alone SFC based FD	Seawater ($C_{i,0} = 3.5wt\%$)	No	0.014	6.7–13.3	0.6–1.2
Rane and Padiya[15]	Stand-alone PFC based FD	Seawater ($C_{i,0} = 3.5wt\%$)	No	1	9–11	0.8–1.0
Rich et al.[97]	Stand-alone PFC based FD	Seawater ($C_{i,0} = 3.5wt\%$)	No	0.0000015	N. A.	N. A.
Zambrano et al.[62]	Integration of FFFC, FT and BFC based FD	Seawater ($C_{i,0} = 3.5wt\%$)	No	0.743	11.5	1.1
Chang et al.[68]	Stand-alone SFC based FD	Seawater ($C_{i,0} = 3.5wt\%$)	Yes	0.000525	N. A.	N. A.
Wang and Chung[70]	SFC based FD and DCMD hybrid system	Seawater ($C_{i,0} = 3.5wt\%$)	Yes	0.01144	4.6	0.4

Note: N. A.: Not available.

thermodynamically accurate (no exergy destruction calculations of individual processes of a desalination system) that avoids any misunderstandings regarding the energy status derived from different sources. The thermodynamic limit (*TL*) of energy consumption ranges from 0.7 to 0.85kWh_{pe}/m^3 for salinity range 3 to 4.5% solute by weight at 25°C[98]. For normal seawater at 3.5% solute by weight at 25°C, the *TL* is 0.78kWh_{pe}/m^3 or 2.8 kJ/kg[98,99]. The subscript 'pe' represents primary energy. The efficiency of a desalination plant/system is called as performance ratio (*PR*). For an vaporization-based desalination plant/system, *PR* is defined as the ratio of latent heat of vaporization of the saltwater to the energy input. Mathematically, *PR* is expressed as:

$$PR_{vap} = \frac{H_{lg}}{3.6\left\{\left(\frac{kWh_{ele}}{m^3}\right) + \left(\frac{kWh_{th}}{m^3}\right)\right\}} \tag{14}$$

where H_{lg} is the latent heat of vaporization of the saltwater (kJ/kg), kWh_{ele}/m^3 is the electrical energy consumption, kWh_{th}/m^3 is the thermal energy consumption, and the constant 3.6 is the unit conversion factor. Since different derived energies are not the same in terms of quality (work potential) so conventional *PR* is a misleading concept for different desalination technologies comparison[100]. Shahzad et al.[101] proposed the universal performance ratio (*UPR*) method to evaluate the desalination processes on a common platform based on primary energy consumption. Primary energy refers to the energy available from a source that constitutes 100% exergy[102]. In *UPR*, the derived energies are multiplied with respective conversion factors to convert into primary energies; those can be then added to calculate the total input to the desalination process. For an vaporization-based desalination plant, *UPR* is defined as:

$$UPR_{vap} = \frac{H_{lg}}{3.6\left\{CF_1\left(\frac{kWh_{ele}}{m^3}\right) + CF_2\left(\frac{kWh_{th}}{m^3}\right) + CF_3\left(\frac{kWh_{renew}}{m^3}\right)\right\}} \tag{15}$$

where, CF_1 is the conversion factor for electricity to the primary energy, CF_2 is the conversion factor for thermal input to the primary energy and CF_3 for renewable to primary energy. The conversion factors calculations are based on exergy destruction across the components corresponding to primary fuel exergy. The derived specific energies are converted to the equivalent primary energy based on these conversion factors. Based on the thermodynamic limit (*TL*) of energy consumption, UPR_{vap} is 828 for seawater desalination[101]. For freeze desalination plants, *UPR* can be defined as:

$$UPR_{freeze} = \frac{H_{ls}}{3.6\left\{CF_1\left(\frac{kWh_{ele}}{m^3}\right) + CF_2\left(\frac{kWh_{th}}{m^3}\right) + CF_3\left(\frac{kWh_{renew}}{m^3}\right)\right\}} \tag{16}$$

where H_{ls} is the latent heat of freezing of the saltwater (kJ/kg). Based on the thermodynamic limit (*TL*) of energy consumption, UPR_{freeze} is 120. In literature, 4.6kWh/m^3 is the minimum value of energy consumption reported by Wang and Chung[70] for a hybrid (integrating MD and SFC based FD) method utilizing LNG cold energy. The plant efficiency is merely 16.3% of the thermodynamic limit ($UPR_{freeze}=120$).

FUTURE RESEARCH RECOMMENDATIONS AND CONCLUSIONS

Future research recommendations

There are many areas in which improvements need to be done:

1. The essential requirement for developing FD technology is understanding the process of crystal growth and separation of concentrated saltwater from the ice under various operating conditions. Furthermore, saltwater desalination involves simultaneous heat and mass transfer[103,104] which is difficult to study analytically. Numerical methods enable the analysis and visualization of different transport processes (like simultaneous heat and mass transfer) by using a computer.

The use of computational fluid dynamics (CFD) modeling can be a valuable tool for this purpose. This kind of investigation can aid in designing a novel crystallizer with enhanced heat and mass transfer (concentrated saltwater separation) during the FD process.

2. In practice, the optimum duration of the process exists, for which thawed ice meet the potable and/or irrigation water salinity limits and initiate a new batch/process. A heat and mass transfer study can predict the optimum duration of the FD process[105,106]. No study is reported in the literature concerning the prediction of optimum process duration for direct contact and indirect contact (SFC and FFFC) FD methods.
3. In literature, most of the studies on FD are limited to desktop experiments with significantly less potable water production capacity. Only a few pilot-scale studies were communicated in literature. Widespread lab-scale studies are needed to make sure the upscaling for the commercial feasibility.
4. In many studies, crystallization, ice separation, and post-treatment of the ice (or thawing) were carried out separately. This increases the capital and maintenance costs. Novel crystallizers that include crystallization, separation of ice from the concentrated saltwater, and post-treatment of the ice in a single unit should be developed. It is necessary to emphasize that layer freeze-concentration based FD methods involve crystallization, ice separation from the concentrated saltwater, and thawing in a single unit. Furthermore, PFC and FFFC based FD methods utilizing saltwater circulation (decreases the concentration gradient adjacent to the ice-liquid interface) can significantly increase potable water production capacity if upscaled appropriately. Hence, these method needs to be explored extensively.
5. Most of the crystallizers operate in batch mode. The crystallizers can be configured appropriately to ensure uninterrupted potable/irrigation water production.
6. Using FD, the partial desalination of brine (a by-product of a seawater desalination process) needs to be explored to reduce its salinity near seawater. The salinity-reduced brine waste (10,000–30,000 ppm TDS) can be used as a supplementary water resource for oil/gas exploration[107] and desalination plants[86], where brine is partially desalinated to supplied back into the seawater desalination unit as feed water.
7. The energy consumption and operating cost of potable/irrigation water from seawater or brackish water can be reduced significantly by removing the latent heat gained by the ice and liquid separately[108].
8. LNG cold energy can fulfill the energy requirement of the freeze desalination process. Furthermore, LNG can generate electrical energy, which can power a stand-alone FD plant and other desalination methods (RO, FO, ED, MD, MSF, MVC, MED, AD, and HDH) in the hybrid system. Other potential methods to support energy consumption include renewable energy and waste heat, producing the electric power required to operate an FD method.
9. Efforts should be directed towards hybrid methods (integration of the FD method with other desalination methods) wherein the energy consumption is supported by LNG cold energy, renewable energy and waste heat. This kind of hybridization would make the FD technology highly energy efficient. In the hybrid system, the design and optimization of the integrated unit would be beneficial compared to the separate design and optimization of each desalination method. Moreover, a detailed thermodynamic analysis is necessary in order to improve and/or optimize the system performance.
10. It is necessary to explore the concept of co-location for LNG regasification terminals, and FD plants. The concept of co-location is extensively used in the reverse osmosis based desalination industry. A typical example is co-locating a reverse osmosis desalination system with an existing power plant[107,109]. The co-location permits the RO system to use the existing facilities of the power plant to reduce its environmental effects and capital cost[107,110].
11. The use of corrosion-resistant material such as Cu-Ni alloy, Al alloy, epoxy coated steel, polyvinylidene fluoride as a cooling surface can increase the life of an FD system and decrease the maintenance and water production cost. The thermal conductivity of material influences the heat transfer during the process. Hence, a heat transfer study should be carried out to select the appropriate corrosion-resistant material.
12. The method of freeze-concentration is widely practised in the pharmaceutical and food industry to a remarkable extent. The commercial processes and equipment applied in the pharmaceutical and food industry should be explored for applications in the desalination industry.
13. There has always been natural unwillingness to accept new technology, mainly when adequate results are obtained from the existing methods. This attitude of the desalination industry towards FD methods should be changed by identifying and conveying the environmental and economic benefits.

CONCLUSIONS

This paper provided an overview of advances in freeze desalination (stand-alone and hybrid) technologies based on the scientific articles published from 2011 to 2021. Furthermore, the paper discussed the future focus areas for research and development. The review shows that FD methods can produce freshwater from seawater and brackish water. The parameters that need to be optimized are the mixing of rejected salt from ice into the liquid phase, the growth of ice crystals, liquid subcooling, and ice seeding/post-treatment of the obtained ice. All FD methods have less potable water production capacity than membrane-based and vaporization-based desalination methods. However, the electrical energy consumption and cost of potable water production for SFC based FD method without latent heat recovery were less than MD and HDH methods, similar to the MED and MSF methods, and higher than the membrane-based desalination method without phase change. The electrical energy consumption and cost for stand-alone SFC and PFC based freeze desalination with latent heat recovery was reported close to the conventional RO method. The hybrid method involving the integration of the suspension FD method with membrane distillation utilizing LNG cold energy consumed less energy than the conventional RO method. Both stand-alone and hybrid methods can be powered by LNG cold energy, renewable energy, and waste heat. An appropriately upscaled stand-alone/hybrid system utilizing heat recovery, LNG cold energy, and renewable energy can emerge as a low-cost desalination alternative in the future.

DATA AVAILABILITY

The author declare that no datasets were generated during the current study.

CODE AVAILABILITY

The author declare that no computer code was written or developed during the current study.

Received: 19 October 2021; Accepted: 23 February 2022;
Published online: 19 April 2022

REFERENCES

1. Ghalavand, Y., Hatamipour, M. S. & Rahimi, A. A review on energy consumption of desalination processes. *Desalination Water Treat.* **54**, 1526–1541 (2015).
2. Jones, E., Qadir, M., van Vliet, M. T. H., Smakhtin, V. & Kang, S. The state of desalination and brine production: a global outlook. *Sci. Total Environ.* **657**, 1343–1356 (2019).
3. Shahzad, M., W.,Burhan, M., Ang, L. & Ng, K. C. Energy-water-environment nexus underpinning future desalination sustainability. *Desalination* **413**, 52–64 (2017).
4. Li, L., Shi, W. & Yu, S. Research on forward osmosis membrane technology still needs improvement in water recovery and wastewater treatment. *Water* **12**, 107 (2020).
5. Ahmed, M., Kumar, R., Garudachari, B. & Thomas, J. P. Performance evaluation of a thermo-responsive polyelectrolyte draw solution in a pilot scale forward osmosis seawater desalination system. *Desalination* **452**, 132–140 (2019).
6. Xing, Y. et al. Performance study of a pilot-scale multi-effect vacuum membrane distillation desalination plant. *Desalination* **403**, 199–207 (2017).
7. Lee, C., Park, K., Woo, C., C., Y., Choi, J. S. & Kim, J. O. A pilot study of spiral-wound air gap membrane distillation process and its energy efficiency analysis. *Chemosphere* **239**, 124696 (2020).
8. Drioli, E., Ali, A. & Macedonio, F. Membrane operations for process intensification in desalination. *Appl. Sci.* **7**, 1–14 (2017).
9. Mohamed, A., S., A., Ahmed, M., S., Maghrabie, H. M. & Shahdy, A. G. Desalination process using humidification-dehumidification technique: a detailed review. *Int. J. Energy Res* **45**, 3698–3749 (2021).
10. Al-Karaghouli, A. & Kazamerski, L. L. Energy consumption and water production cost of conventional and renewable-energy-powered desalination processes. *Renew. Sustain. Energy Rev.* **24**, 343–356 (2013).
11. Bernardes, A., M., Rodrigues, M. A. S. & Ferreira, J. Z. Electrodialysis and water reuse: novel approaches. Ch. 3 (Springer-Verlag, Berlin, 2013).
12. Ahmed, F. E., Hashaikeh, R. & Hilal, N. Hybrid technologies: the future of energy efficient desalination - a review. *Desalination* **495**, 114659 (2020).
13. Narayan, G. P. et al. The potential of solar-driven humidification –dehumidification desalination for small-scale decentralized water production. *Renew. Sustain. Energy Rev.* **14**, 1187–1201 (2010).
14. Ahmed, F., E., Khalil, A. & Hilal, N. Emerging desalination technologies: current status, challenges and future trends. *Desalination* **517**, 115183 (2021).
15. Rane, M. V. & Padiya, Y. S. Heat pump operated freeze-concentration system with tubular heat exchanger for seawater desalination. *Energy Sustain. Dev.* **15**, 184–191 (2011).
16. Mtombeni, T. et al. Evaluation of the performance of a new freeze desalination technology. *Int. J. Environ. Sci. Technol.* **10**, 545–550 (2013).
17. Randall, D., G., Nathoo, J. & Lewis, A. E. A case study for treating a reverse osmosis brine using eutectic freeze crystallization - approaching a zero-waste process. *Desalination* **266**, 256–262 (2011).
18. Yadav, A., Labhasetwar, P. K. & Shahi, V. K. Membrane distillation crystallization technology for zero liquid discharge and resource recovery: Opportunities, challenges and futuristic perspectives. *Sci. Total Environ.* **806**, 150692 (2022).
19. Mullin, J. W. Crystallization. Ch. 5 (Butterworth-Heinemann, Oxford, 2001)
20. Vrbka, L. & Jungwirth, V. Brine rejection from freezing salt solutions: a molecular dynamics study. *Phys. Rev. Lett.* **95**, 148501–148504 (2005).
21. Gu, X., Suzuki, T. & Miyawaki, O. Limiting partition coefficient in progressive freeze concentration. *J. Food Sci.* **70**, 546–551 (2005).
22. Luo, C., Chen, W. & Han, W. Experimental study on factors affecting the quality of ice crystal during the freezing concentration for the brackish water. *Desalination* **260**, 231–238 (2010).
23. Vuist, J., E., Boom, R. M. & Schutyser, M. A. I. Solute inclusion and freezing rate during progressive freeze-concentration of sucrose and maltodextrin solutions. *Dry. Technol.* **38**, 1285–1293 (2020).
24. Rice, W. & Chau, D. S. C. Freeze desalination using hydraulic refrigerant compressors. *Desalination* **109**, 157–164 (1997).
25. Liu, L., Miyawaki, O. & Nakamura, K. Progressive freeze-concentration of model liquid food. *Food Sci. Technol. Int.* **3**, 348–352 (1997).
26. Ding, Z. et al. Concentration of apple juice with an intelligent freeze concentrator. *J. Food Eng.* **256**, 61–72 (2019).
27. Casas-Forero, N., Orellana-Palma, P. & Petzold, G. Influence of block freeze concentration and evaporation on physicochemical properties, bioactive compounds and antioxidant activity in blueberry juice. *Food Sci. Technol.* **40**, 387–394 (2020).
28. Samsuri, S., Amran, N. A. & Jusoh, M. Spiral finned crystallizer for progressive freeze concentration process. *Chem. Eng. Res. Des.* **104**, 280–286 (2015).
29. Habib, B. & Farid, M. Freeze concentration of milk and saline solutions in a liquid-solid fluidized bed: Part I. Experimental. *Chem. Eng. Process.: Process Intensif.* **46**, 1400–1411 (2007).
30. Jaster, H. et al. Enhancement of antioxidant activity and physicochemical properties of yogurt enriched with concentrated strawberry pulp obtained by block freeze concentration. *Food Res. Int.* **104**, 119–125 (2018).
31. Gao, W. & Shao, Y. Freeze-concentration for removal of pharmaceutically active compounds in water. *Desalination* **249**, 398–402 (2009).
32. Weber, D. & Hubbuch, J. Raman spectroscopy as a process analytical technology to investigate biopharmaceutical freeze concentration processes. *Biotechnol. Bioeng.* **118**, 4708–4719 (2021).
33. Samsuri, S. et al. Progressive freeze-concentration for volume reduction of produced water and biodiesel wastewater. *Chem. Eng. Technol.* **42**, 1764–1770 (2019).
34. Miyawaki, O., Liu, L. & Nakamura, K. Effective partition constant of solute between ice and liquid phases in progressive freeze concentration. *J. Food Sci.* **63**, 1–4 (1998).
35. Amran, N. et al. Review: parametric study on the performance of progressive cry-concentration system. *Chem. Eng. Comm.* **203**, 957–975 (2016).
36. Sanchez, J., Hernandez, E., Auleda, J. M. & Raventos, M. Freeze concentration of whey in a falling-film based pilot plant: process and characterization. *J. Food Eng.* **103**, 147–155 (2011).
37. Gulfo, R. et al. Multi-plate freeze concentration: recovery of solutes occluded in the ice and determination of thawing time. *Food Sci. Technol. Int.* **20**, 405–419 (2014).
38. Moreno, F., L., Raventos, M., Hernandez, E. & Ruiz, Y. Block freeze-concentration of coffee extract: effect of freezing and thawing stages on solute recovery and bioactive compounds. *J. Food Eng.* **120**, 158–166 (2014).
39. Najim, A. Discussion on "B. Kalista, H. Shin, J. Cho, A. Jang, Current development and future prospect review of freeze desalination, Desalination, 447(2018), 167–181" and "A. Eghtesad, M. Salakhi, H. Afshin, S. Hannani, Numerical investigation and optimization of indirect freeze desalination, Desalination, 481 (2020), 114378" *Desalination* **504**, 114958(2021).
40. Braga, S. L. & Viskanta, R. Solidification of a binary solution on a cold isothermal surface. *Int. J. Heat. Mass Transf.* **33**, 745–754 (1990).
41. Fernández-Torres, M., Ruiz-Beviá, J., F., Rodríguez-Pascual, M. & von Blottnitz, H. Teaching a new technology, eutectic freeze crystallization, by means of a solved problem. *Educ. Chem. Eng.* **7**, e163–e168 (2012).
42. Randall, D. G. & Nathoo, J. A succinct review of the treatment of reverse osmosis brines using freeze crystallization. *J. Water Process Engg.* **8**, 186–194 (2015).
43. Kalista, B., Shin, H., Cho, J. & Jang, A. Current development and future prospect review of freeze desalination. *Desalination* **447**, 167–181 (2018).
44. Fioriti, D. et al. LNG regasification and electricity production for port energy communities: Economic profitability and thermodynamic performance. *Energy Convers. Manag* **238**, 114128 (2021).
45. Zhang X. R. & Dincer I. Energy Solutions to Combat Global Warming. Ch. 3 (Springer International Publishing, Switzerland, 2017)
46. Kanbur, B., Xiang, B., Dubey, L., S., Choo, F. & Duan, F. Cold utilization systems of LNG: a review. *Renew. Sustain. Energy Rev.* **79**, 1171–1188 (2017).
47. He, T., Nair, S., K., Babu, P., Linga, P. & Karimi, I. A. A novel conceptual design of hydrate-based desalination (HyDesal) process by utilizing LNG cold energy. *Appl. Energy* **222**, 13–24 (2018).
48. He, T., Chong, Z., Zheng, R., J., Ju, Y. & Linga, P. LNG cold energy utilization: prospects and challenges. *Energy* **170**, 557–568 (2019).
49. Erlbeck, L. et al. Investigation of the depletion of ions through freeze desalination. *Desalination* **407**, 93–102 (2017).
50. Liu, Y. et al. Desalination of seawater by spray freezing in a natural draft tower. *Desalination* **496**, 114700 (2020).
51. Zvinowanda, C. M. et al. Process optimization of freeze desalination of brine using HybridICE^{TM} pilot plant. *Desalin. Water Treat.* **52**, 6315–6324 (2014).
52. Erlbeck, L., Wössner, D., Kunz, T., Rädle, M. & Methner, F. J. Investigation of freeze crystallization and ice pressing in a semi-batch process for the development of a novel single-step desalination plant. *Desalination* **448**, 76–86 (2018).
53. Erlbeck, L. et al. Investigation of a novel scraped surface crystallizer with included ice-pressing section as new purification technology. *Sep. Purif. Technol.* **228**, 115748 (2019).
54. Shin, H., Kalista, B., Jeong, S. & Jang, A. Optimization of simplified freeze desalination with surface scraped freeze crystallizer for producing irrigation water without seeding. *Desalination* **452**, 68–74 (2019).
55. Sahu, P., Krishnaswamy, S. & Pande, N. K. Process intensification using a novel continuous U-shaped crystallizer for freeze desalination. *Chem. Eng. Process. - Process. Intensif.* **153**, 107970 (2020).
56. Abdelmoaty, H., M., Mahgoub, A. U. & Abdeldayem, A. W. Performance analysis of salt reduction levels in indirect freeze desalination system with and without magnetic field exposure. *Desalination* **508**, 115021 (2021).
57. Rich, A. et al. Sea water desalination by dynamic layer melt crystallization: parametric study of the freezing and sweating steps. *J. Cryst. Growth* **342**, 110–116 (2012).
58. Ab Hamid, F. H. et al. Desalination of seawater through progressive freeze-concentration using a coil crystallizer. *Water Sci. Tech. - Water Sup.* **15**, 625–631 (2015).

59. Fujioka, R., Wang, L., P., Didbiba, G. & Fujita, T. Application of progressive freeze concentration for desalination. *Desalination* **319**, 33–37 (2013).
60. Moharramzadeh, S., Ong, S., K., Alleman, J. & Cetin, K. S. Parametric study of the progressive freeze concentration for desalination. *Desalination* **510**, 115077 (2021).
61. Williams, P., M., Ahmad, M. & Connolly, B. S. Freeze desalination: an assessment of an ice maker machine for desalting brines. *Desalination* **308**, 219–224 (2013).
62. Zambrano, A., Ruiz, Y., Hernandez, E., Raventos, M. & Moreno, F. L. Freeze desalination by the integration of falling film and block freeze-concentration techniques. *Desalination* **436**, 56–62 (2018).
63. Baayyad, I., Hassani, N. S. A. & Bounahmidi, T. Evaluation of the energy consumption of industrial hybrid seawater desalination process combining freezing system and reverse osmosis. *Desalin. Water Treat.* **56**, 2593–2601 (2015).
64. Han, D., He, W., F., Ji, C. & Huang, L. Thermodynamic analysis of a novel evaporation and crystallization system based on humidification processes at ambient temperature. *Desalination* **439**, 108–118 (2018).
65. Xie, C. et al. A direct contact type ice generator for seawater freezing desalination using LNG cold energy. *Desalination* **435**, 293–300 (2018).
66. Ong, C. W. & Chen, C. L. Technical and economic evaluation of seawater freezing desalination using liquefied natural gas. *Energy* **181**, 429–439 (2019).
67. Cao, W., Beggs, C. & Mujtaba, I. M. Theoretical approach of freeze seawater desalination on flake ice maker utilizing LNG cold energy. *Desalination* **355**, 22–32 (2015).
68. Chang, J., Zuo, J., Lu, K. & Chung, T. S. Freeze desalination of seawater using LNG cold energy. *Water Res* **102**, 282–293 (2016).
69. Lin, W., Huang, M. & Gu, A. A seawater freeze desalination prototype system utilizing LNG cold energy. *Int. J. Hydrog. Energy* **42**, 18691–18698 (2017).
70. Wang, P. & Chung, T. S. A conceptual demonstration of freeze desalination-membrane distillation (FD-MD) hybrid desalination process utilizing liquefied natural gas (LNG) cold energy. *Water Res* **46**, 4037–4052 (2012).
71. Chang, J., Zuo, J., Lu, K. J. & Chung, T. S. Membrane development and energy analysis of freeze desalination-vacuum membrane distillation hybrid systems powered by LNG regasification and solar energy. *Desalination* **449**, 16–25 (2019).
72. Lu, K., J., Cheng, Z. L., Chang, J., Luo, L. & Chung, T. S. Design of zero liquid discharge desalination (ZLDD) systems consisting of freeze desalination, membrane distillation, and crystallization powered by green energies. *Desalination* **458**, 66–75 (2019).
73. Lu, K. & Chung T. Membrane distillation. Ch. 11 (CRC press, New York, 2019)
74. Eghtesad, A., Afshin, H. & Hannani, S. K. Energy, exergy, exergoeconomic, and economic analysis of a novel power generation cycle integrated with seawater desalination system using the cold energy of liquified natural gas. *Energy Convers. Manag* **243**, 114352 (2021).
75. Han, S., Rhee, Y. W. & Kang, S. P. Investigation of salt removal using cyclopentane hydrate formation and washing treatment for seawater desalination. *Desalination* **404**, 132–137 (2017).
76. Han, S., Shin, J., Y., Rhee, Y. W. & Kang, S. P. Enhanced efficiency of salt removal from brine for cyclopentane hydrates by washing, centrifuging, and sweating. *Desalination* **354**, 17–22 (2014).
77. Mandri, Y. et al. Parametric study of the sweating step in the seawater desalination process by indirect freezing. *Desalination* **269**, 142–147 (2011).
78. Badawy, S. M. Laboratory freezing desalination of seawater. *Desalin. Water Treat.* **57**, 11040–11047 (2016).
79. Tan, W., Jia, Z., Li, C., Gao, X. & Cheng, C. Study on sea ice desalination technology via centrifuge. *Desalin. Water Treat.* **54**, 2969–2975 (2015).
80. Han, S., Kim, W., Lee, Y., Jun, B. M. & Kwon, Y. Investigation of Hydrate-induced Ice Desalination (HIID) and its application to a pre-treatment of reverse osmosis (RO) process. *Desalination* **395**, 8–16 (2016).
81. Yang, H., Zhan, Z., Yao, Y. & Sun, Z. Influence of gravity-induced brine drainage on seawater ice desalination. *Desalination* **407**, 33–40 (2017).
82. Erlbeck, L. et al. Commercial feasibility of a new freeze crystallization plant for small scale potable water production. *Desalin. Water Treat.* **105**, 23–34 (2018).
83. Tang, W., Tao, J., Wang, J., Liu, C. & Zhang, H. Sea ice desalination under gravity using microwave heating. *Desalination* **430**, 159–164 (2018).
84. Tang, W., Shi, P., Wang, J. & Zhang, H. Sea ice centrifugal desalination based on microwave heating. *Desalination* **449**, 1–5 (2019).
85. Mavukkandy, M., O., Chabib, C. M., Mustafa, I., Al Ghaferi, A. & Al Marzooqi, F. Brine management in desalination industry: from waste to resources generation. *Desalination* **472**, 114187 (2019).
86. Morillo, J. et al. Comparative study of brine management technologies for desalination plants. *Desalination* **336**, 32–49 (2014).
87. Giwa, A., Dufour, V., Al Marzooqi, F., Al Kaabi, M. & Hasan, S. W. Brine management methods: recent innovations and current status. *Desalination* **407**, 1–23 (2017).
88. Amy, G. et al. Membrane-based seawater desalination: present and future prospects. *Desalination* **401**, 16–21 (2017).
89. Randall, D. G. & Nathoo, J. Resource recovery by freezing: a thermodynamic comparison between a reverse osmosis brine, seawater and stored urine. *J. Water Process Eng.* **26**, 242–249 (2018).
90. Chen, Q. et al. A zero liquid discharge system integrating multi-effect distillation and evaporative crystallization for desalination brine treatment. *Desalination* **502**, 114928 (2021).
91. Bardi, U. Extracting minerals from seawater: an energy analysis. *Sustainability* **2**, 980–992 (2010).
92. Melak, F., Ambelu, A., Astatkie, H., Du Laing, G. & Alemayehu, E. Freeze desalination as point-of-use water defluoridation technique. *Appl. Water Sci.* **9**, 34 (2019).
93. Conde, M., M., Rovere, M. & Gallo, P. Molecular dynamics simulations of freezing-point depression of TIP4P/2005 water in solution with NaCl. *J. Mol. Liq.* **261**, 513–519 (2018).
94. Yen, Y. C. Review of thermal properties of snow, ice and sea ice, USA Cold Regions Research and Engineering Laboratory, Hanover, NH (1981).
95. Mtombeni, T. et al. Evaluation of the performance of a new freeze desalination technology. *Int. J. Environ. Sci. Technol.* **10**, 545–550 (2013).
96. Chen, D., Zhang, C., Rong, H., Wei, C. & Gou, S. Experimental study on seawater desalination through supercooled water dynamic ice making. *Desalination* **476**, 114233 (2020).
97. Rich, A. et al. Freezing desalination of sea water in a static layer crystallizer. *Desalin. Water Treat.* **13**, 120–127 (2010).
98. Ng, K., C., Shahzad, M. W., Son, H. S. & Hamed, O. A. An exergy approach to efficiency evaluation of desalination. *Appl. Phys. Lett.* **110**, 184101 (2017).
99. Ng, K. C. A thermodynamic platform for evaluating the energy efficiency of combined power generation and desalination plants. *NPJ Clean. Water* **4**, 25 (2021).
100. Jamil, M., A. Shahzad, M. W. & Zubair, S. M. A comprehensive framework for thermo-economic analysis of desalination systems. *Energy Convers. Manag* **222**, 113188 (2020).
101. Shahzad, M., W.,Burhan, M., Son, H. S., Oh, S. J. & Ng, K. C. Desalination processes evaluation at common platform: a universal performance ratio (UPR) method. *Appl. Therm. Eng.* **134**, 62–67 (2018).
102. Shahzad, M., W.,Burhan, M. & Ng, K. C. A standard primary energy approach for comparing desalination processes. *NPJ Clean. Water* **2**, 1 (2019).
103. Jayakody, H., Al-Dadah, R. & Mahmoud, S. Computational fluid dynamics investigation on indirect contact freeze desalination. *Desalination* **420**, 21–33 (2017).
104. Eghtesad, A., Salakhi, M., Afshin, H. & Hannani, S. K. Numerical investigation and optimization of indirect freeze desalination. *Desalination* **481**, 114378 (2020).
105. Zhang, H., Janajreh, I., Ali, M. I. H. & Askar, K. Freezing desalination: Heat and mass validated modeling and experimental parametric analysis. *Case Stud. Therm. Eng.* **26**, 101189 (2021).
106. Najim, A. & Krishnan, S. A similarity solution for heat transfer analysis during progressive freeze-concentration based desalination. *Int. J. Therm. Sci.* **172**, 107328 (2022).
107. Mokheimer, E. M. A. et al. A comprehensive review of thermal enhanced oil recovery: techniques evaluation. *ASME J. Energy Resour. Technol.* **141**, 030801 (2019).
108. Najim, A. & Krishnan, S. Experimental and theoretical investigation of a novel system for progressive freeze-concentration based desalination process. *Chem. Eng. Process. – Process Intensif.*, **173**, 108821 (2022).
109. Mei, Y. & Tang, C. Y. Co-locating reverse electrodialysis with reverse osmosis desalination: synergies and implications. *J. Membrane Sci.* **539**, 305–312 (2017).
110. Voutchkov, N. Seawater desalination costs cut through power plant co-location. *Filtr. Sep.* **41**, 24–26 (2004).

ACKNOWLEDGEMENTS

The author would like to thank Prof. Shankar Krishnan, Department of Mechanical Engineering, IIT Bombay, India, for motivation and support while writing the manuscript.

COMPETING INTERESTS

The authors declare no competing interests.

ADDITIONAL INFORMATION

Correspondence and requests for materials should be addressed to Abdul Najim.

Reprints and permission information is available at http://www.nature.com/reprints

Publisher's note Springer Nature remains neutral with regard to jurisdictional claims in published maps and institutional affiliations.

Open Access This article is licensed under a Creative Commons Attribution 4.0 International License, which permits use, sharing, adaptation, distribution and reproduction in any medium or format, as long as you give appropriate credit to the original author(s) and the source, provide a link to the Creative Commons license, and indicate if changes were made. The images or other third party material in this article are included in the article's Creative Commons license, unless indicated otherwise in a credit line to the material. If material is not included in the article's Creative Commons license and your intended use is not permitted by statutory regulation or exceeds the permitted use, you will need to obtain permission directly from the copyright holder. To view a copy of this license, visit http://creativecommons.org/licenses/by/4.0/.

© The Author(s) 2022